AN INVESTIGATION OF THE AERODYNAMICS AND COOLING OF A HORIZONTALLY-OPPOSED ENGINE INSTALLATION

S. J. MILEY

1977

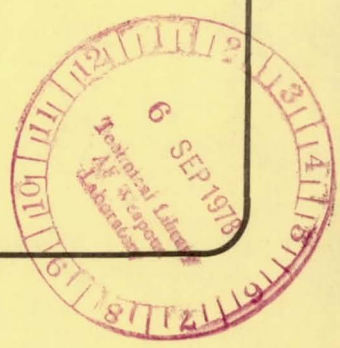

LAND SEA AIR SPACE

SOCIETY OF AUTOMOTIVE ENGINEERS, INC.
400 Commonwealth Drive, Warrendale, Pa. 15096

An Investigation of the Aerodynamics and Cooling of a Horizontally-Opposed Engine Installation

S. J. Miley
Dept. of Aerophysics and Aerospace Engrg.,
Mississippi State Univ.

Society of Automotive Engineers

Business Aircraft Meeting
Century II, Wichita
March 29 - April 1, 1977

770467

770467

An Investigation of the Aerodynamics and Cooling of a Horizontally-Opposed Engine Installation

S. J. Miley
Dept. of Aerophysics and Aerospace Engrg.,
Mississippi State Univ.

This work supported by NASA LRC,
NASA Grant Number NSG-1083

AIR-COOLED ENGINES ARE, by definition, engines whose operating temperatures are controlled by dissipating the generated heat to the surrounding air-mass. Engines of small power output such as those used for lawnmowers, chainsaws, etc., are sufficiently cooled through radiation and convection. Heat removal from the higher power output engines which are used to propel automobiles and aircraft, on the other hand, requires a sustained mass flow of cooling air about the engine. The mechanism through which the cooling flow is maintained is dependent on the particular type of vehicle. Automobiles and helicopters must operate at speeds which are too low to generate the required flow by motion through the surrounding air mass. Accordingly, these vehicles utilize a fan, driven directly from the engine, with associated ducting to produce the necessary cooling flow. Fixed wing aircraft, however, generally operate at velocities through the air mass which are sufficient to generate an adequate cooling flow.

The necessity of requiring a coolant flow to dissipate engine heat, whether the coolant is liquid or air, directly or indirectly absorbs some of the generated power. The applications which require fans or pumps are evident direct power utilizations. In the case of fixed wing aircraft, the power is absorbed indirectly through the specific drag contributions of the air-cooling system to the total aircraft drag. In other words, the power required to propel the aircraft at a given velocity can be subdivided and proportionally related to the drag contributions of the different parts of the aircraft, i.e., wings, fuselage, tail, cooling system, etc., and accounted for accordingly. It is common practice (1-4)* to relate, in particular, the power increments absorbed by cooling systems, protuberances and other items which clutter up the aircraft's exterior to corresponding increments in airspeed which would be gained if the corresponding power increments were otherwise available. Consequently, one can speak in terms of a door handle costing 0.5 knots, a flap hinge costing 2 knots, and a cooling system costing 6.5 knots. Reducing or eliminating the drag components associated with external protuberances is relatively straight forward aerodynamically, although, increased mechanical complexity and corresponding higher production costs may enter the problem. Reducing or minimizing the drag component associated with the cooling system

*Numbers in parentheses designate References at end of paper.

ABSTRACT

A research program to investigate the aerodynamics of reciprocating aircraft engine cooling installations is discussed. Current results from a flight test program are presented concerning installation flow measurement methods. The influence of different inlet designs on installation cooling effectiveness and efficiency are described.

is, at present, a somewhat more difficult problem, primarily due to an effective lack of applicable aerodynamic data for the elements which make up the system. The term "effective" is used here to indicate that while, in some cases, applicable data may exist, there has, until now, been no effort to dig it out, put it into a useable form, and disseminate it.

For the past two years, a program of exploratory research into cooling drag has been underway at the Raspet Flight Research Laboratory, Mississippi State University. The principle objective of the program is the development and dissemination of a "Cooling Installation Design Handbook" for general aviation aircraft. This is being accomplished through a coordinated effort of literature research and experimental flight research. The purpose of this paper is to report some of the results of the flight research program which are presently available.

BACKGROUND

Air-cooled reciprocating aircraft engines exist in two basic geometries, radial and in-line. The in-line group can be further subdivided into pure in-line, Vee and horizontally-opposed. The distinction between these geometries is important when considering the external and internal aerodynamics of their respective cooling installations. A distinction is also made between two types of air mass-flow cooling; velocity and pressure. Velocity cooling denotes the use of relatively high flow velocities about the body, i.e., cooling by blowing on it. Pressure cooling denotes cooling by forcing relatively low velocity flow through heat-dissipating-fin passages on the exterior of the body. A pressure difference across the body is required to sustain the cooling mass flow. Aircraft engines are designed for pressure cooling.

Figure 1 shows a horizontally-opposed engine with a ground test stand cooling installation typical of current practice. The blower supplies cooling air to a duct leading to the engine face. A diffuser and plenum are located above the engine to convert the velocity head to pressure and provide a uniform distribution over the engine. A pressure difference is thus created across the engine which forces sufficient mass flow through the cooling fins. In terms of delivering cooling air to the engine, the resulting temperature distribution and cooling characteristics, this installation is the ideal case or baseline to which actual aircraft installations should be referenced. Effectively, the cooling characteristics of the engine are designed for the situation in Figure 1, i.e., no velocity cooling, pressure cooling only, and a uniform pressure and flow at the engine face. To the extent that actual aircraft installations deviate from this, cooling problems can arise.

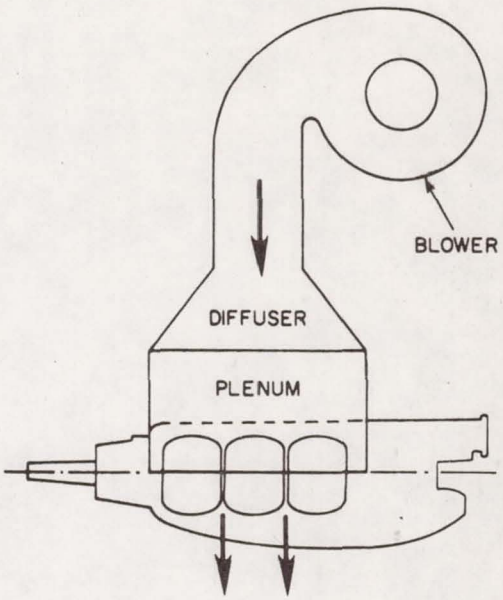

Fig. 1 - Ground test cooling installation

Another point concerning Figure 1 must be made. The illustration implies that all horizontally-opposed engines are designed for a cooling flow direction from top to bottom or so called "downdraft cooling." Engines are also available with the flow direction from bottom to top, or "updraft cooling." In either case, the term engine face is applied to the high pressure flow side of the engine.

Engine cooling requirements are given in terms of cooling air mass flow and temperature for pertinent engine operating conditions and cylinder temperatures. Since an accurate measurement of mass flow is impractical for aircraft installations, the mass flow is related to the corresponding pressure difference across the engine. The relationship between mass flow and engine pressure difference is a function of operating altitude and temperature rise in the cooling flow across the engine. It is current practice to develop a sea level curve of mass flow versus pressure difference and to generate the corresponding altitude curves by dividing the mass flow by the Standard Atmosphere sea level pressure ratio. Figure 2 shows an example of engine cooling requirements data.

Figure 3 illustrates examples of aircraft installations for radial, in-line, Vee and horizontally-opposed engines. The functional objectives of these installations are stated as follows:

To baffle the exterior planform of the engine so that only the cooling fin passages remain between the high and low pressure sides.

To utilize the available dynamic pressure in an efficient manner to supply high pressure uniformly distributed cooling flow to the engine face.

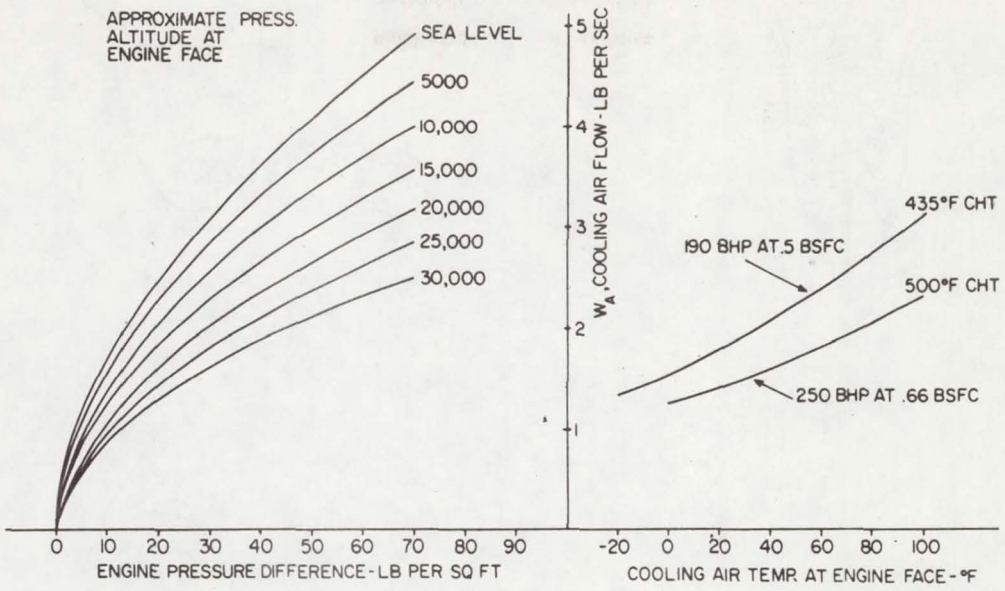

Fig. 2 - T10-540-L1AD Engine cooling requirements

To exhaust the cooling flow efficiently downstream.

To provide an effective pumping mechanism on the low pressure side for high power, low speed flight conditions.

To accomplish the above with a minimum of external losses and drag.

The aerodynamic approach taken to meet these objectives is strongly influenced by the basic engine geometry. The first distinction is whether the plane of the engine face is perpendicular to the flight path, as in the case of the radials, or parallel to the flight path, as in the case of the in-lines. For radial installations, the engine face is orientated so that it receives the flight dynamic pressure directly. Aerodynamic analyses and design here are more concerned with external flow problems such as controlling the pressure distribution across the engine face over the angle-of-attack range of the aircraft, and avoiding flow separation and supercritical flow (Mach > 1) on the cowl exterior. In-line installations, on the other hand, require both external and internal aerodynamic analyses. The primary problem here is that an efficient inlet/diffuser/plenum system must be incorporated into the fuselage or nacelle to recover the flight dynamic pressure and deliver the cooling flow to the engine face. A further distinction can be made between the pure in-line and Vee geometries which are amenable to installations with a single inlet/diffuser, and the horizontally opposed geometries, whose installations mostly employ two inlets (commonly called bug-eyes).

The importance of distinguishing between these engine geometries and associated installation aerodynamics lies with the problem of utilizing currently existing data and analyses to develop efficient horizontally-opposed installations for general aviation aircraft. Over 95% of the information available deals with radial engines, and was developed in the period 1930-1945. The remainder concerns pure in-line and Vee installations developed during World War II. The in-line data is definitely more valuable because the installation aerodynamics are essentially the same as the horizontally-opposed. The prime source of in-line information in this country is the Ranger engine and installation development program of the 1940's. Reference (5) presents a good summary of this work. The current experimental phase of the Mississippi State cooling drag program has been influenced strongly by the Ranger installation research effort.

EXPERIMENTAL PROGRAM DESCRIPTION

The cooling drag experimental program at the Raspet Flight Research Laboratory is a systematic investigation of the pertinent design parameters and associated aerodynamics of a horizontally-opposed engine installation. The investigation is conducted as a flight research program utilizing a Piper PA-41P Aztec shown in Figure 4. The aircraft was donated to Mississippi State University by Piper Aircraft for this program. The aircraft is powered by two Lycoming TIO-540-L1AD turbo-supercharged engines which were donated by Avco Lycoming. Also the propellers were donated by Hartzell Propeller. This aircraft has been committed to research on general aviation propulsion system problems, and has

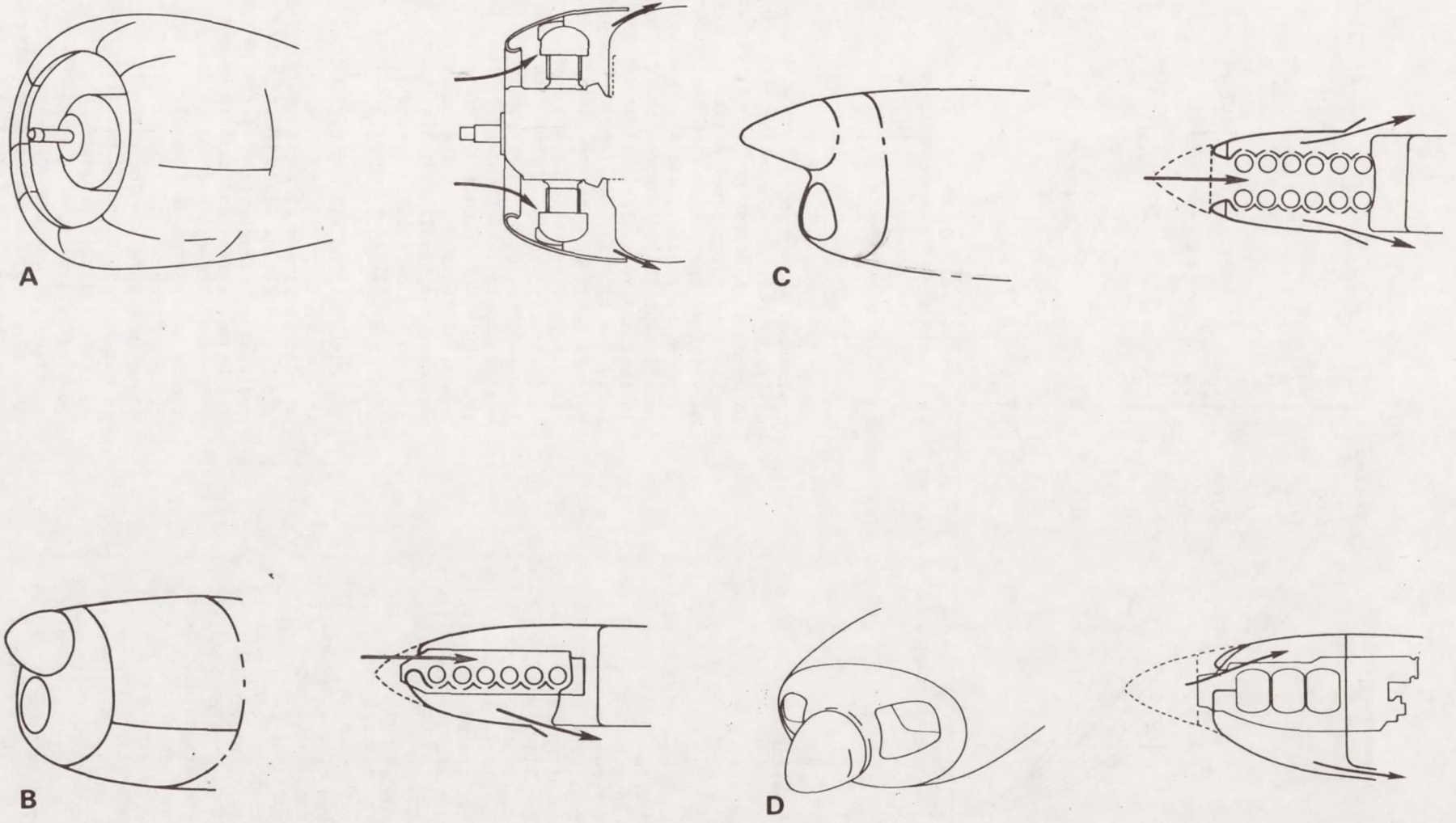

Fig. 3A-D - Aircraft engine cooling installations - A: radial, B: in-line, C: Vee, and D: horizontally-opposed

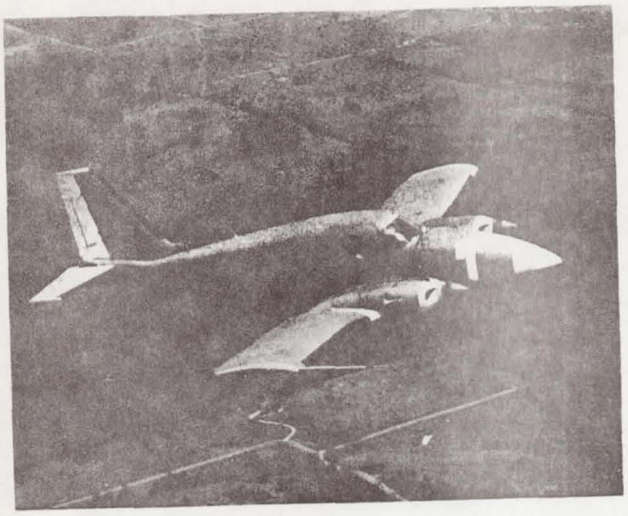

Fig. 4 - Piper PA-41P Propulsion System Research Vehicle

accordingly been redesignated as PSRV (Propulsion System Research Vehicle).

INSTALLATION RESEARCH - The right nacelle of the PA-41P has been extensively modified for this program. The modifications are illustrated in Figure 5. The original nacelle utilized louvers on the upper and lower surfaces to exhaust the cooling flow. The oil cooler was mounted internally with an external inlet. There were no baffling between the exit cooling flows of the engine and oil cooler so that the lower plenum pressure was a function of the pressure differences across both. For the modified test nacelle, the oil cooler was mounted external to the nacelle and its cooling flow separated from that of the engine. Also, accessory cooling, such as the alternator and magnitos, was separated and provided with individual inlets. The purpose here was to measure the cooling mass flow of the engine only and correlate it with the pressure difference across the engine. A Kiel tube propeller wake rake

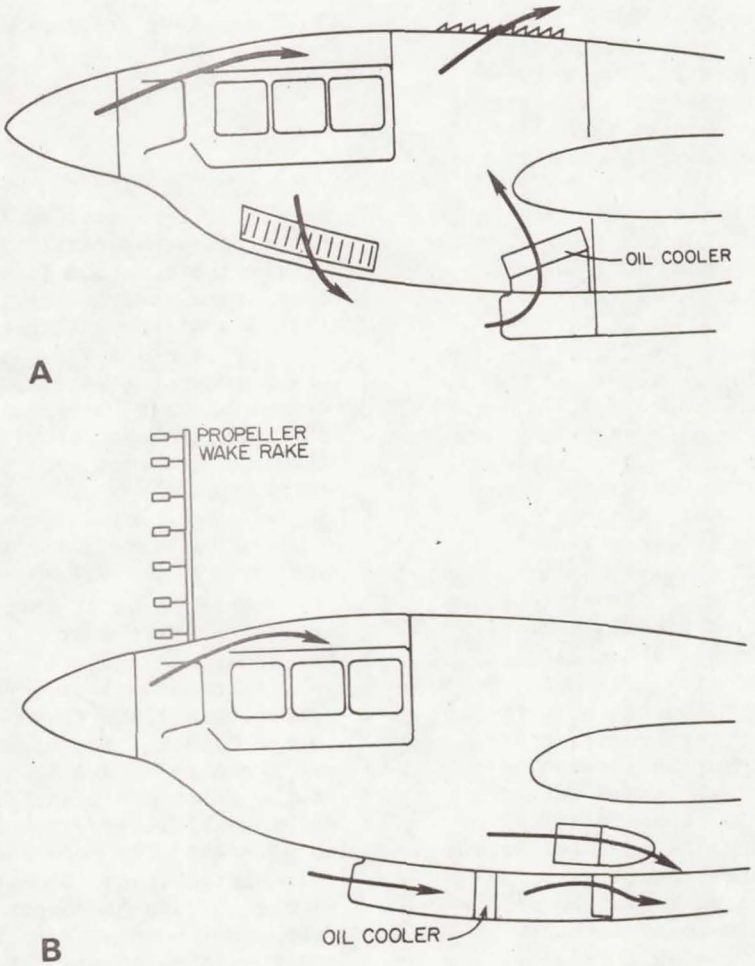

Fig. 5A&B - Nacelle modifications for propulsion system research - A: original PA-41P; B: current PSRV

was mounted as shown to measure the total pressure distribution behind the propeller.

The installation was divided into specific components to be studied. These components are inlet, plenum and exit. To date, only inlet design parameters have been investigated. Plenum and exit design parameters will be investigated during spring/summer 1977.

The function of the inlet is to recover the available flow dynamic pressure and deliver the high pressure flow to the plenum in a uniform manner. Ideally, this should be accomplished with no internal or external flow separation. Inlets are classified as either two-dimensional, as in the case of wing leading edge intakes, or three-dimensional, as in the case of jet engine intakes. As an aerodynamic shape, inlets behave similarly to airfoil sections. They have internal and external pressure distributions which are similar to airfoil pressure distributions. These distributions change with angle of attack of the inlet similar to airfoil distributions. Consequently, an inlet is subject to stall (flow separation) both internally and externally, as is the airfoil, at high positive and negative angles of attack. Changes in the inlet velocity ratio (ratio of the flow velocity at the inlet throat to the free stream velocity) produce effects on the pressure distributions similar to changes in angle of attack. Low velocity ratios tend to cause external flow separation and high velocity ratios tend to cause internal flow separation. The former is generally known as spillage drag.

The inlets selected to be tested were of the Kuchmann A-20 family in Reference (6). Two inlet sections were chosen, one for a velocity ratio $v_i/v_o = 0.6$, and the other for $v_i/v_o = 0.3$. The inlet sections are shown in Figure 6. The inlet throat area was determined according to the procedure given in Reference (3). These inlets are axisymmetric designs and the axisymmetric shape was maintained as much as possible while incorporating the inlets into the nose cowl. This was done in order to measure the change in the inlet pressure distributions from the basic axisymmetric shape as affected by the nose cowl and the propeller. From these inlets, three nose cowls were fabricated and tested. The installation design parameters were inlet velocity ratio and longitudinal location relative to the propeller plane. Those with the forward position were also tested with and without an internal diffuser. The fourth nose cowl tested was with the original PA-41P inlet. This inlet is similar to the conventional Aztec inlet except it has a larger intake area and, as a consequence, has smaller radii of curvature on the upper and lower lips. The four test nose cowls are shown in Figures 7-10. Table 1 identifies each of the inlets as they are referenced in this paper.

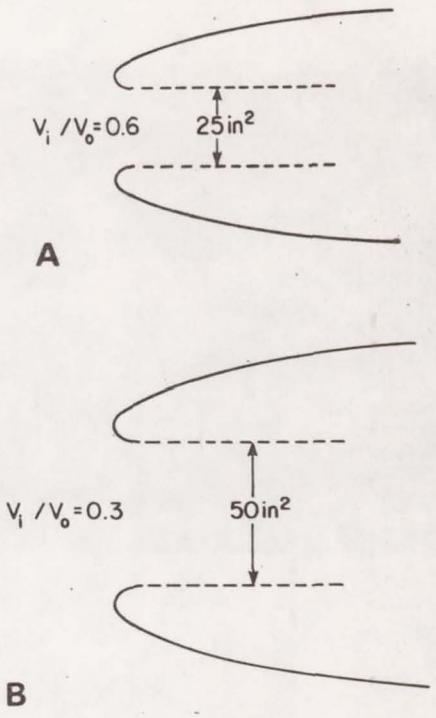

Fig. 6 - Test inlet shapes - A: design velocity ratio $v_i/v_o = 0.6$; B: design velocity ratio $v_i/v_o = 0.3$

INSTRUMENTATION - The PSRV instrumentation system will be divided into two parts and described separately. The first part consists of the installation flow pressure and temperature probes and sensors, and the second part consists of the data acquisition system.

Installation Flow Instrumentation - The objectives of the installation flow instrumentation were to measure the flow pressure distributions and total pressure losses through the installation, and to evaluate different techniques for measuring the engine pressure difference. Total pressure surveys, utilizing Kiel tubes, were taken at the rear of the inlet duct in front of the leading cylinders, across the upper plenum at three longitudinal stations, and in the exit duct. The inlet Kiel tube rakes are shown in Figure 11. Evident also in Figure 11b is the propeller governor which obstructs approximately one-third of the duct area leading to the plenum. The upper plenum Kiel tube rakes are shown in Figure 12. Kiel tubes were used in the inlet and plenum surveys because they are insensitive to flow angularity errors up to 60 degrees. The more common pitot tubes are insensitive up to 10 degrees. Also shown in Figure 12, are the upper plenum temperature probes which consist of a thermocouple sensor and radiation shield. The radiation shields were made from chrome-plated copper tubing commonly used in bathroom fixture plumbing.

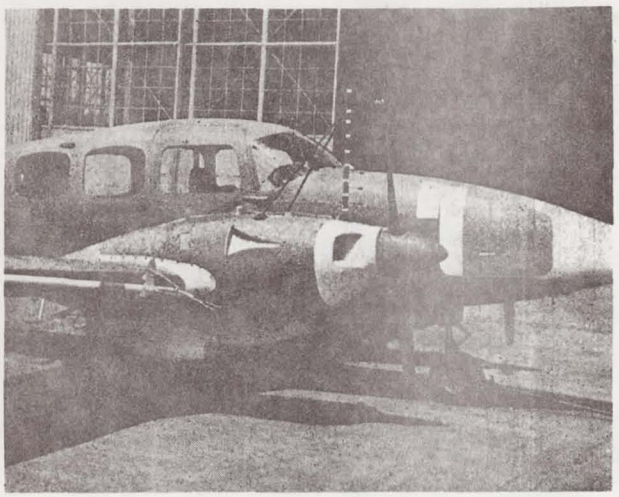

Fig. 7A - Standard PA-41P (STD) inlet - front view

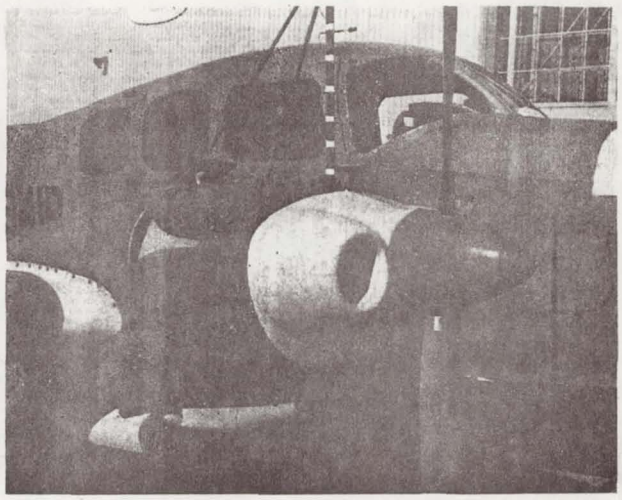

Fig. 8A - Design velocity ratio v_i/v_o = 0.3, forward location (0.3F) inlet - front view

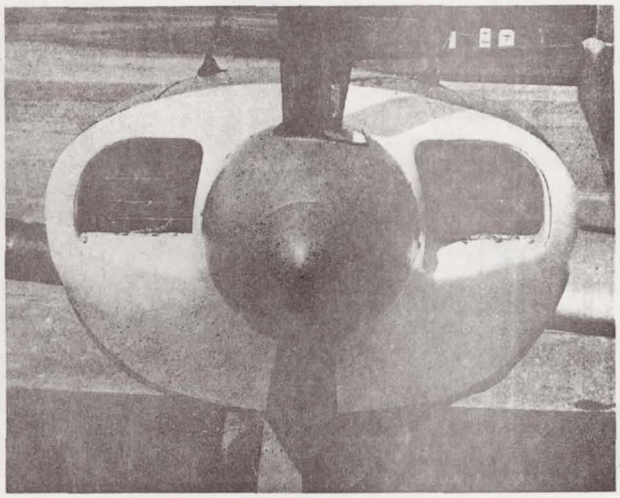

Fig. 7B - Standard PA-41P (STD) inlet - side view

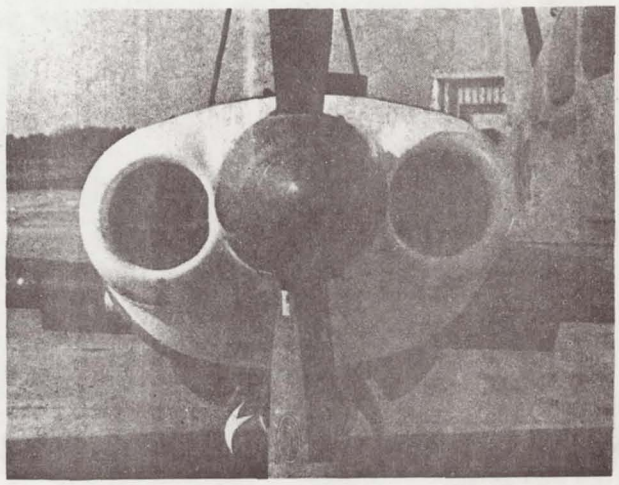

Fig. 8B - Design velocity ratio v_i/v_o = 0.3, forward location (0.3F) inlet - side view

The pressure distribution on the engine face and the pressure difference across the engine were measured by a number of different probes and methods. Representative techniques of both airframe and engine manufacturers were included. Figure 13 illustrates the various probe configurations and locations. All probes shown in Figure 13a except (#1) are 1/16 inch diameter open end total pressure tubes. The tube opening was internally chamfered to a 60 degree included angle. This increased the probe angularity insensitivity to approximately 28 degrees. The vertical positions of these probes are given in Figure 13c. The cylinder barrel tubes (#2) and cylinder head tubes (#3) were located vertically on the center line of the cylinder. Cylinder head tubes (#4) were located 3/8 inch below the local fin height on the exhaust stack side of the cylinder. Cylinder head tubes (#5) were located between adjacent cylinders flush with the top of the local fins. Referring to Figure 12a, the (#5) tubes were effectively recessed below the engine face proper, but were still exposed the engine face pressure without fin passage losses. Probes (#1) of Figures 13a and 13d consist of a brass roundhead machine screw inserted through the intercylinder baffle at the base of the barrels. The screw is drilled for and fitted with a 1/16 inch tube for connection to a pressure line. The head of the screw is filled and smoothed. This type of probe is commonly called a "baffle button" and from now on will be referred to as such. Piccolo tubes, shown in Figures 13b and

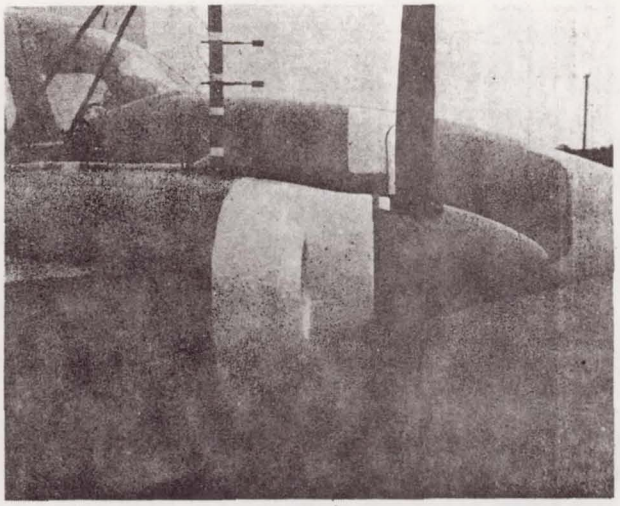

Fig. 9A - Design velocity ratio v_i/v_o = 0.3, aft location (0.3A) inlet - front view

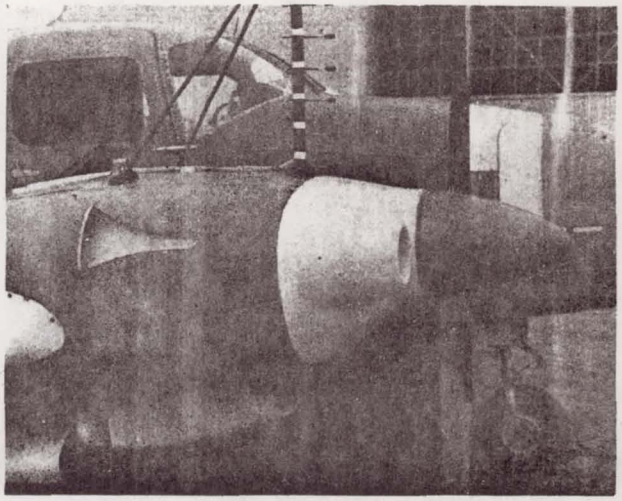

Fig. 10A - Design velocity ratio v_i/v_o = 0.6, forward location (0.6F) inlet - front view

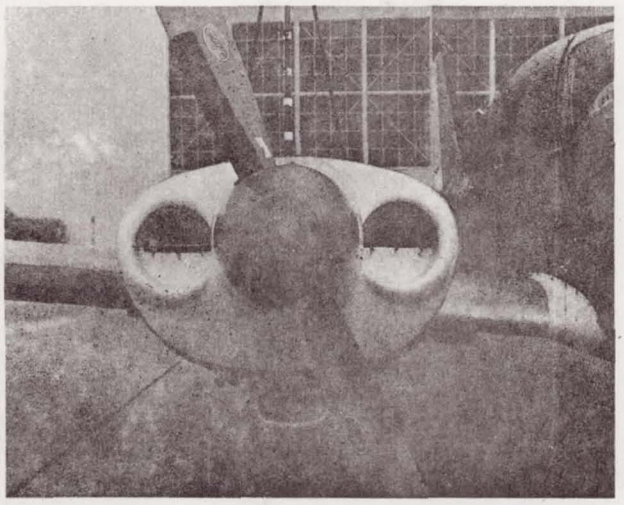

Fig. 9B - Design velocity ratio v_i/v_o = 0.3, aft location (0.3A) inlet - side view

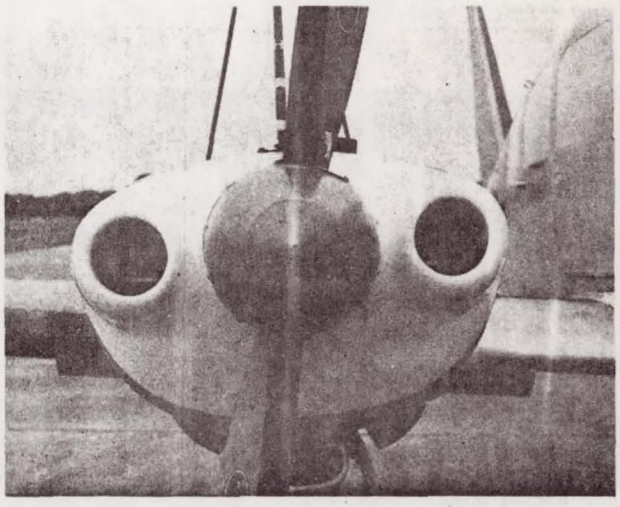

Fig. 10B - Design velocity ratio v_i/v_o = 0.6, forward location (0.6F) inlet - side view

13f were mounted in the upper and lower plenums to provide an integrated or averaged measurement of the static pressure. The assumption here is that if a true plenum exists, then the static and total pressures are the same. The upper plenum static pressure was also measured by multielement pressure belts similar to the kind used in flight test to measure the wing section pressure distribution. As shown in Figure 13g, the belts were attached to the inside upper surface of the top cowl. Hole spacing between belt elements was 2 inches.

The lower plenum static and total pressures are assumed to be the same because of the relatively large volume. The practice used in installation flow analysis is to consider the pressure here as a static pressure. The lower plenum static pressure was measured by four

Table 1 - Cross-Reference of Inlets Tested

Figure	v_i/v_o	Location	Designation
7	0.3	-	STD
8	0.3	Forward	0.3F
9	0.3	Aft	0.3A
10	0.6	Forward	0.6F

different probes. The most common practice is to use total pressure tubes located in the low pressure side of the engine so that they are shielded from any local high velocities. The total-probe configurations used are shown in Figures 13d and 13e. A set of battle shield probes was located in the lower plenum at each of the baffle button positions (probes (#1) in Figure 13a). Fin shield static probes were

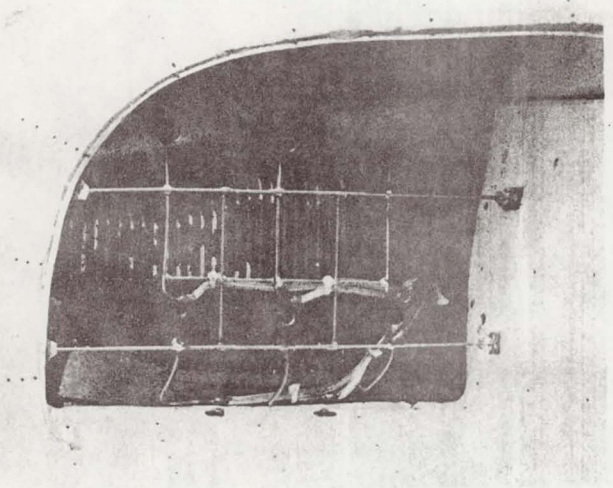

Fig. 11A - Inlet Kiel tube rakes - right (outboard) side

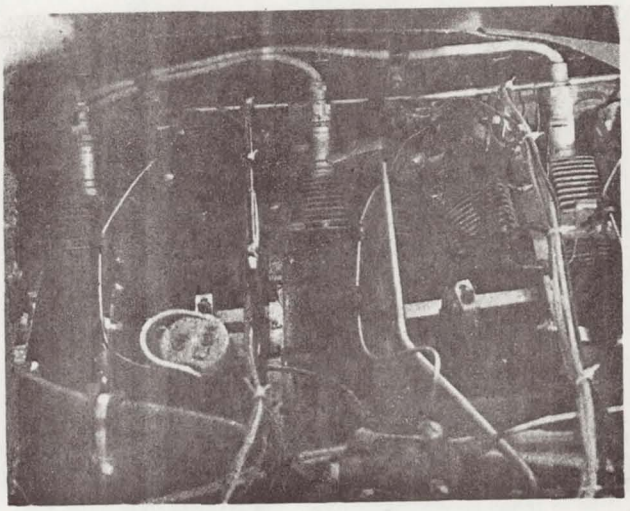

Fig. 12A - Upper plenum Kiel tube rake and temperature probe installation - looking inboard

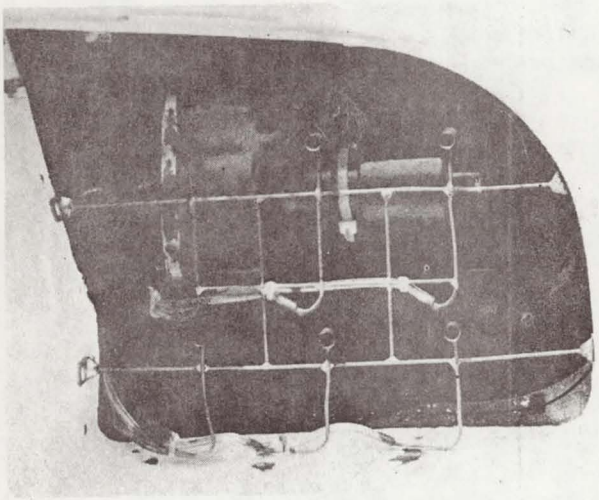

Fig. 11B - Inlet Kiel tube rakes - left (inboard) side

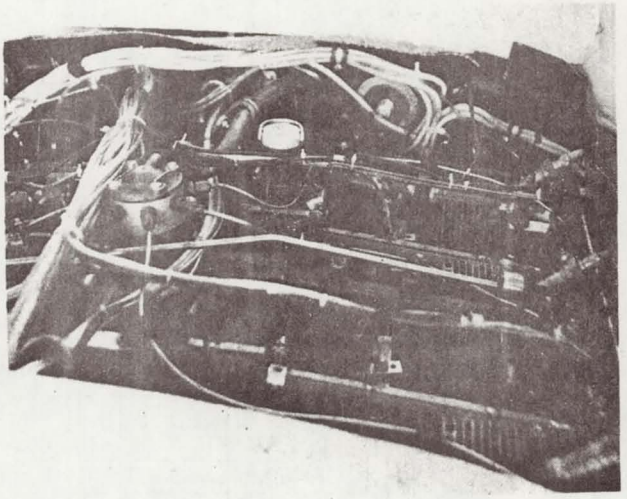

Fig. 12B - Upper plenum Kiel tube rake and temperature probe installation - looking aft

located adjacent to each of the cylinder head tubes (#5). All lower plenum static probes of each configuration were manifolded together to give three distinct averaged measurements. The fourth probe used in the lower plenum was the aforementioned piccolo.

Data Acquisition System - The data acquisition system consists of two elements; an analog recording system with serial multiplexing, and a photo-recording manometer system. A schematic of the analog system is given in Figure 14. A total of 144 channels of pressure data and 48 channels of temperature data, plus airspeed and altitude signals are recorded on a 7 track Lockheed Model 417 recorder. This system is used primarily for installation flow pressure and temperature measurements. For each data point, up to six multiplex cycles are taken, the results averaged and rms errors of each channel computed and checked for anomalies. The analog data is digitized utilizing an HP-2114A minicomputer system and then analyzed on the University's UNIVAC 1106 computer system.

An additional 80 channels of pressure data can be acquired on the PSRV manometer shown in Figure 15. The manometer display is photographed with a 35mm camera using fine grain Panatomic-X film. Lighting is by strobe-flash. The film is read with a desk top microfiche reader rather than a conventional film reader. The microfiche reader gives more contrast and can be used in partial room lighting to assist recording the readings. The photomanometer system is used primarily for external pressure distribution measurements which may change from flight to flight.

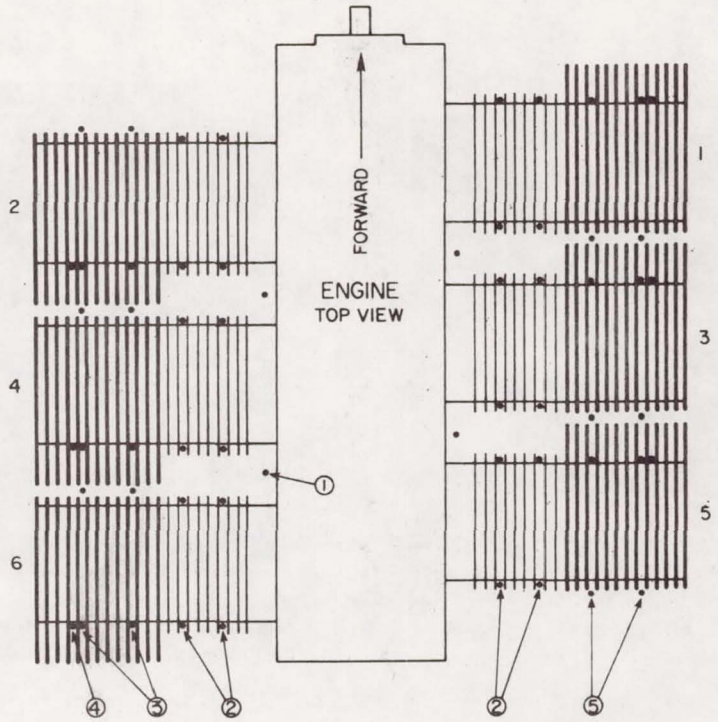

Fig. 13A - Engine pressure difference instrumentation - engine face probe locations

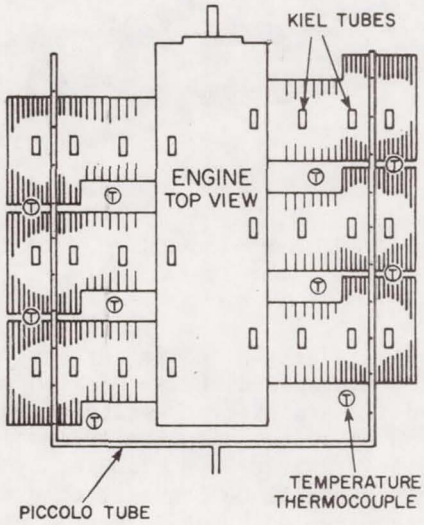

Fig. 13B - Engine pressure difference instrumentation - Kiel tube and piccolo tube locations

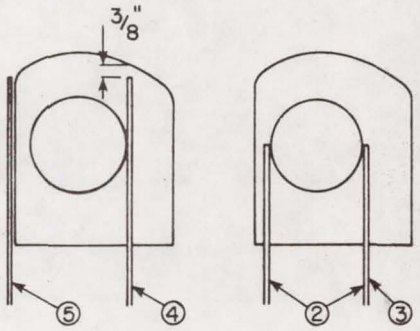

Fig. 13C - Engine pressure difference instrumentation - cylinder probe vertical positions

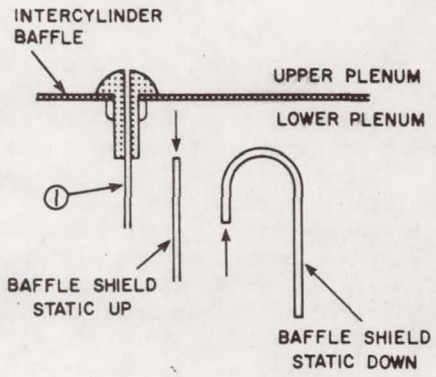

Fig. 13D - Engine pressure difference instrumentation-baffle button and lower plenum static probes

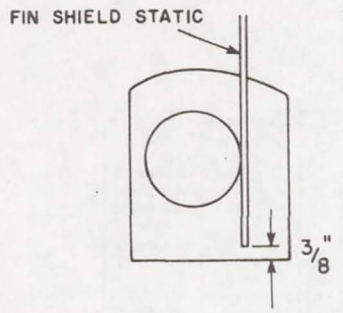

Fig. 13E - Engine pressure difference instrumentation - lower plenum fin shield static probe

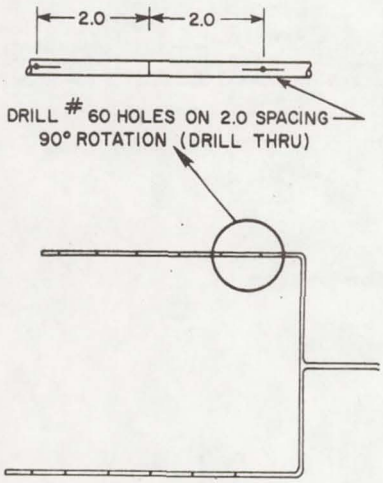

Fig. 13F - Engine pressure difference instrumentation - piccolo tube details

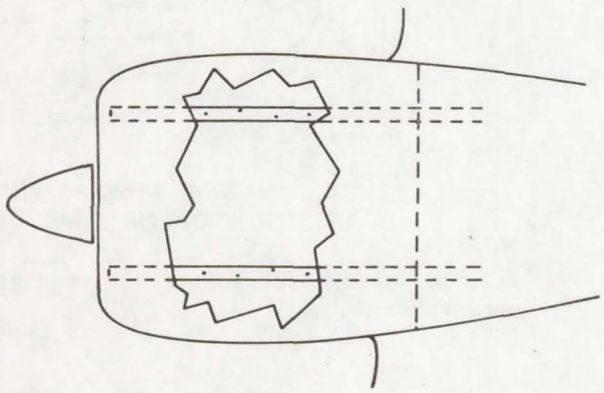

Fig. 13G - Engine pressure difference instrumentation - upper plenum pressure belt installation

RESULTS AND DISCUSSION

Results will be reported for two specific areas of investigation; installation flow measurement techniques, and inlet performance. Pressure notation and points of reference are given in Figure 16.

INSTALLATION INSTRUMENTATION - The purpose of this investigation was to evaluate different probes and techniques for measuring the engine face, and upper and lower plenum pressures.

Lower Plenum Pressure Measurement - Figure 17 presents a comparison of the different lower plenum static pressure probes. The data represent different airspeeds, altitudes and cowl flap settings. The lower plenum statics are referenced to free-stream total pressure for the purpose of measuring the total pressure loss through the installation. Regarding Figure 17, all probes give essentially the same measure. The fin shield probes indicate a static pressure 3% below the piccolo and the baffle shield-down probes indicate 2% above. These differences are explainable by considering the location and orientation of the open end of the particular probes. From the standpoint of simplicity, the piccolo tube is the best method of measuring the lower plenum static pressure.

Engine Face/Upper Plenum Pressure Measurements - If the upper plenum were to function as a true plenum, then the plenum static, total and engine face pressures would be the same. In practice, however, particularly for twin engine aircraft, the plenum volumes are small and the flow velocities are correspondingly high enough to influence the methods by which pressures are measured. The plenum cross sectional area of the PA-41P test aircraft was approximately 100 inches^2 which is also the throat area of the $v_i/v_o = 0.3$ inlets. Accordingly, separate methods were used to measure each of the respective plenum pressures. These methods were described in previous sections of this paper.

Figure 18 presents engine face and plenum static pressure data for two different inlets and two different flight conditions. The data are in the form of pressure coefficients which are defined here to be the static pressure difference between the two points indicated by the subscripts, divided by the free-stream dynamic pressure;

$$C_{P20} = (P_2 - P_0)/q_0 \qquad (1)$$

where

$$q_0 = 1/2\rho_o V_o^2 . \qquad (2)$$

Several observations can be made regarding the data in Figure 18. All pressure measurement methods attempted were subject to flow angularity, orientation and position errors. This is due basically to having finite flow velocities in irregular directions in the plenum. Note that the scatter increases for the climb condition which has a higher mass flow due to

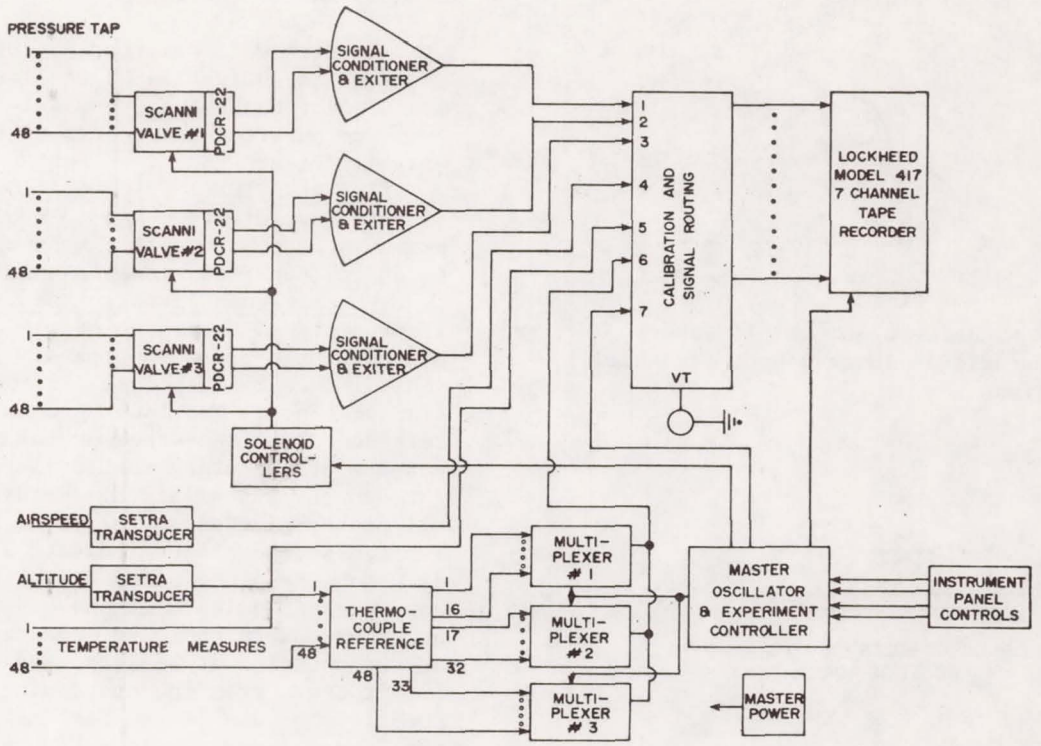

Fig. 14 - PSRV data acquisition system

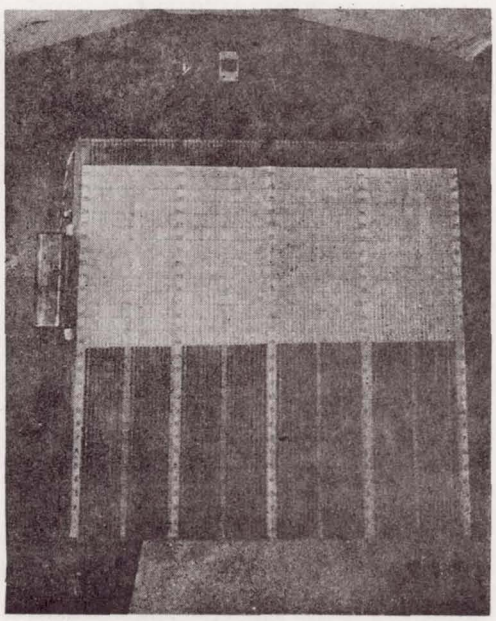

Fig. 15 - PSRV 80-tube photo-manometer

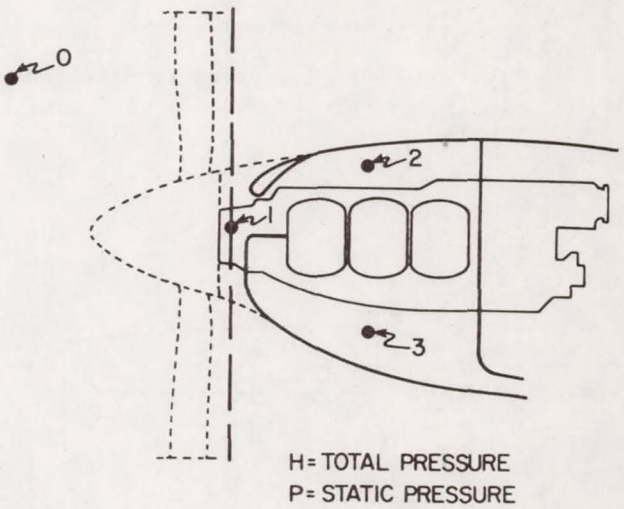

Fig. 16 - Reference points for pressure measurements

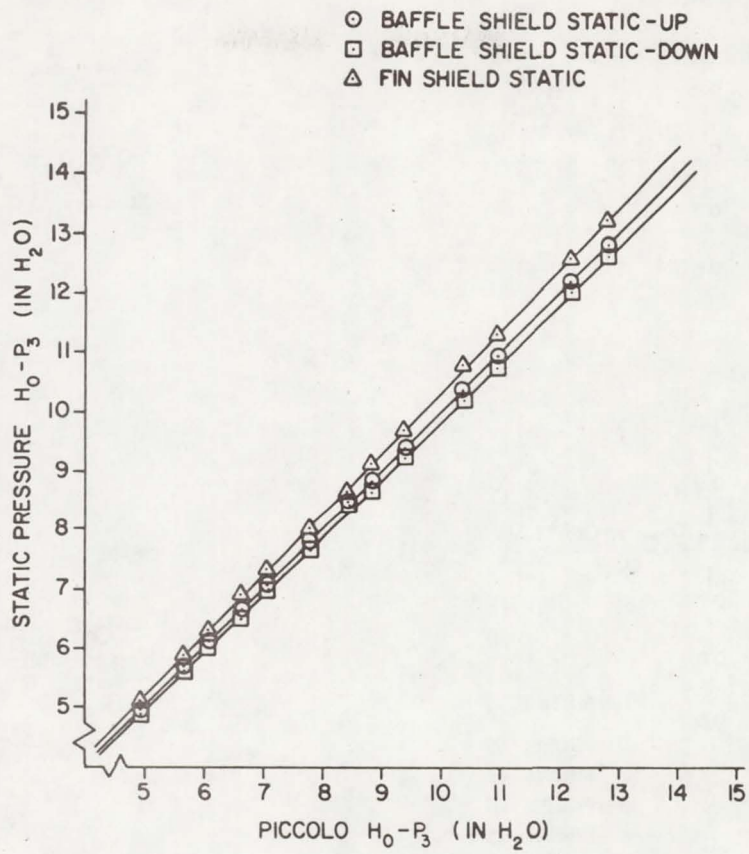

Fig. 17 - Comparison of lower plenum static pressure measurement methods

cowl flap deployment. Also, as will be shown, the propeller exerts a stronger effect on the plenum flow in climb.

The left side of the plenum (cylinders 2-4-6), behaves somewhat differently from the right side (cylinders 1-3-5). This asymmetrical behavior showed itself in a number of different aerodynamic measurements and is believed to be due to inlet flow blockage by the propeller governor (see Figure 11). The scatter pattern is different for each inlet due to changes in the character of the plenum flow.

Engine face pressure is the same as plenum static. There is no effective recovery of the plenum dynamic pressure.

From the standpoint of simplicity and accuracy, the static belt method appears to be the best technique to measure upper plenum static. However, for engines with intake manifolds on the face side or other hardware which cause local changes in plenum volume, the static belt method may be less accurate. This should be tested on an engine of this type and reported. The baffle button probes (#1) also give accurate and reliable data. The piccolo tube indicates low. It is possible that the piccolo reading may be raised through biasing the tube by cutting it short so that it does not extend to the front cylinders.

INLET PERFORMANCE - The effects on the installation of the four inlets tested will be discussed in terms of the resulting total pressure distributions across the plenum and inlets, and of the performance of the installation as a whole. First, however, some results from the external aerodynamics investigation will be presented.

Inlet External Aerodynamics - Figure 19 gives some results from tuft flow visualization studies of the four inlets. The STD inlet in Figure 19a shows flow separation on both sides with the left side exhibiting a larger stalled region. Also, the left corner of the upper lip on the left side indicates separation whereas the corresponding point on the right side is attached. However, when the propeller is stopped, the right side becomes stalled also. This asymmetrical behavior of the inlets is believed to be due to flow blockage effects casued by the propeller governor. Also, external pressure distribution measurements show that the propeller wake flow tends to reduce suction pressure peaks at the inlet lips and thereby tends to reduce the potential for separation.

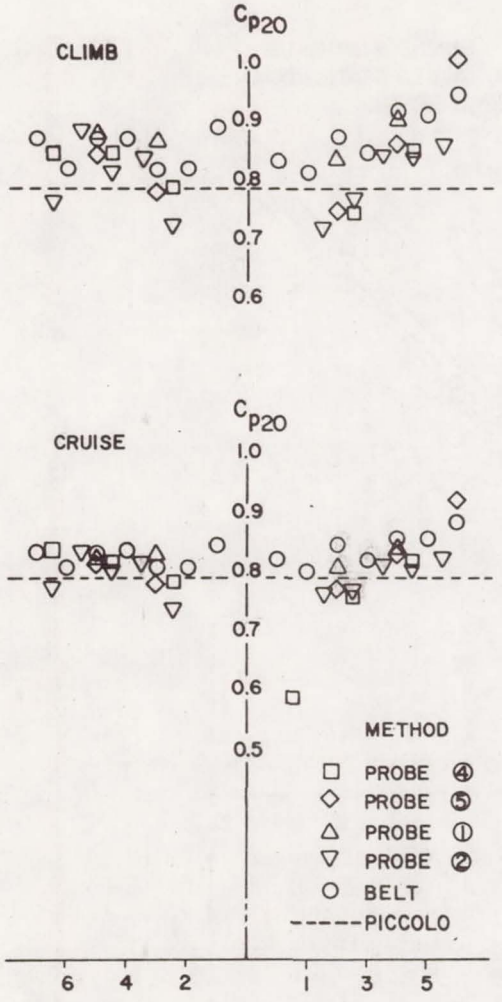

Fig. 18A - Engine face and upper plenum static pressure data - 0.3F inlet

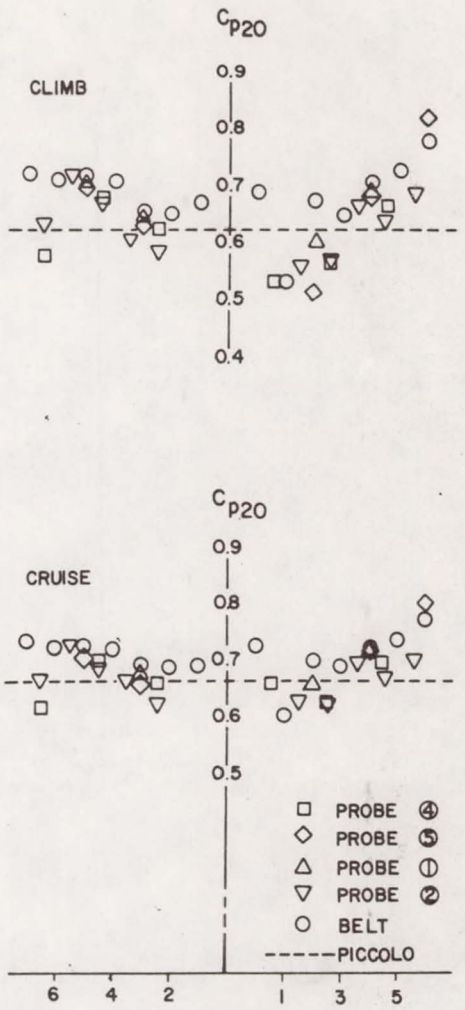

Fig. 18B - Engine face and upper plenum static pressure data - STD inlet

In Figure 19b, the external flow of the 0.3F inlet is well behaved. The lower internal surface of the left side however, shows some local flow reversal, whereas the right side does not.

The 0.3A inlets in Figure 19c are internally stalled over the lower half of the inlet in front of the ramp leading to cylinders 1 and 2. The ramp itself was tufted specifically to test for this. Figure 20 is a post-flight photograph of the inlet showing the tuft locations. Note that the frayed tufts indicate regions of turbulent separation encountered in flight.

In Figure 19d, the 0.6F inlets behaved similarly to the 0.3F inlets. Again, the left side showed some internal flow separation, whereas, the right side did not.

Total Pressure Distributions - Figure 21 presents results of the propeller wake survey and shows a planform view of the nacelle. The pressure coefficient used here differs from the one previously defined by (1) in that the pressure difference is between a total and a static;

$$\overline{C}_{P10} = (H_1 - P_0)/q_0 \qquad (3)$$

where H_1 is the total pressure at 1. Due to the propeller, the inlet sees a variation in total pressure from 0.8 q_0 to about 1.05 q_0 in cruise, and 1.2 q_0 in climb.

Figure 22 gives results from the inlet and plenum total pressure surveys for the different inlets. The presentation shown is a top view of the engine with the inlets in the upper left and right corners of the graph. The respective cylinders are denoted by the numbers 1-6 outside of the graph. The propeller governor is located in the left inlet in front of cylinder number 2.

The 0.3F inlet in Figure 22b gives the highest total pressure recovery in the plenum. The inlet ducts themselves are well behaved as indicated by showing a total pressure distribution similar to the propeller rake. The 0.6F, 0.3A and STD inlets resulted in lower plenum

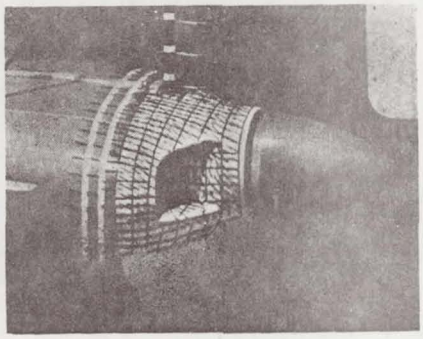

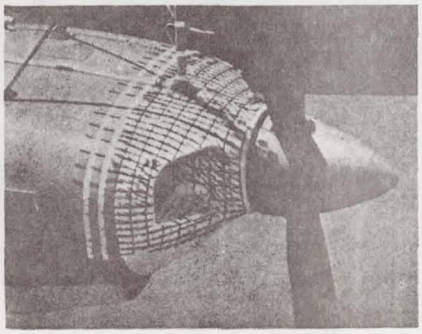

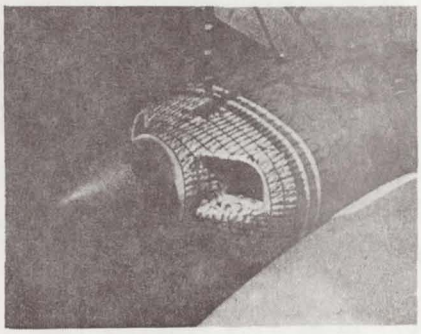

Fig. 19A - Inlet flow visualization studies - STD inlet

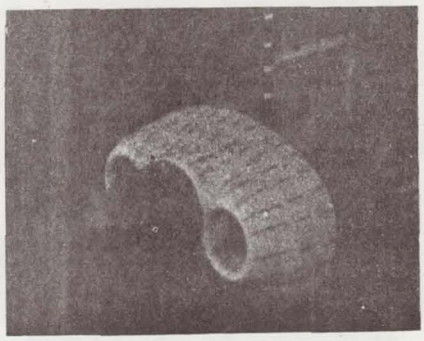

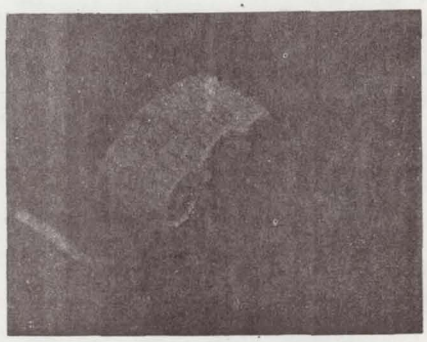

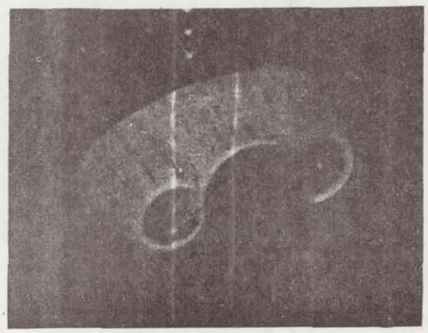

Fig. 19B - Inlet flow visualization studies - 0.3F inlet

total pressures and suffered internal stalling to various degrees. In Figure 22a, the left side of the STD inlet is extensively stalled. In Figures 22c and 22d, stalling on the inlet sides closest to the center line occurs in climb, with the separation region being greater on the left inlet. The tendency for the left inlet to stall is believed, as already mentioned, to be due to flow blockage effects by the propeller governor. Restricting the flow reduces, the inlet velocity ratio which accordingly alters the external and internal inlet pressure distributions so as to result in separation. Separation is also encouraged on the inlet sides closest to the center line by the lower energy flow from the propeller wake near the hub. Data taken with the propeller stopped and feathered shows a more uniform total pressure distribution across the inlets.

Installation Performance - The pressure data presented in this section results from the average of the baffle button probes (#1) for the engine face pressure, and from the piccolo tube for the lower plenum pressure. The data are in pressure coefficient form as previously defined. In this form, the engine face pressure coefficient is the same as the effective plenum pressure recovery, i.e., if

$$C_{P20} = 1$$

then all of the free stream dynamic pressure has been recovered in the plenum. The important fact to consider here is that, neglecting propeller effects and exit pumping mechanisms,

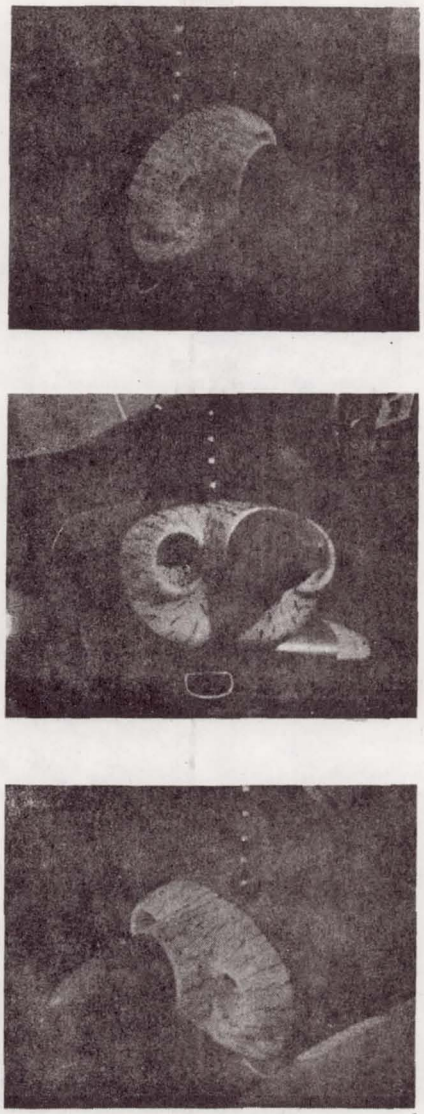

Fig. 19C - Inlet flow visualization studies - 0.3A inlet

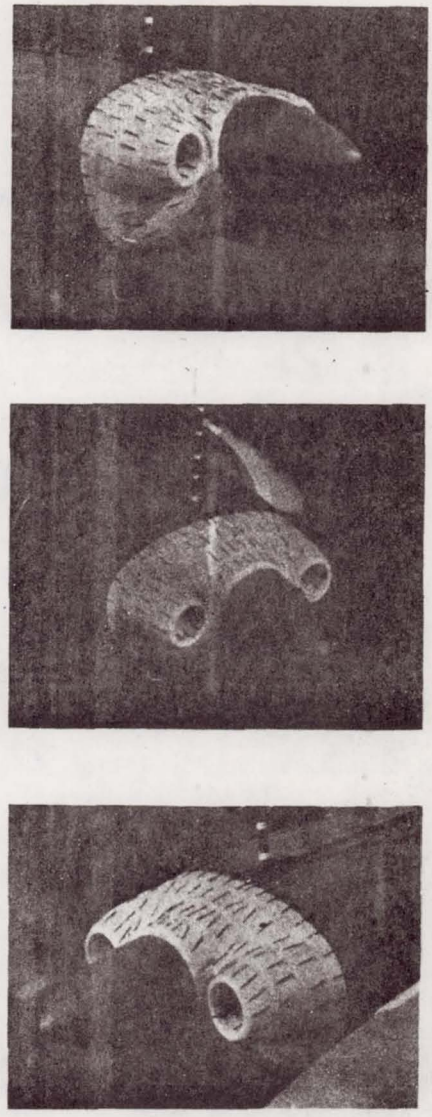

Fig. 19D - Inlet flow visualization studies - 0.6F inlet

the total pressure difference through the installation can not exceed the free stream dynamic pressure.

$$(1 - C_{P20}) + C_{P23} \leq 1 \ . \qquad (4)$$

Figures 23 and 24 present results for the three inlets which were flown over the altitude range of the PA-41P. The data in Figure 23 are for constant equivalent airspeed climbs at constant power with cowl flaps open. The plenum pressure recovery is shown to be independent of altitude while the engine pressure difference decreases with altitude. An analysis of the engine pressure difference variation was performed assuming the mass flow varied as the product of the density and true airspeed. Substituting then the relation for equivalent airspeed gives,

$$W \sim \sqrt{\rho\rho_o}\, V_e \ . \qquad (5)$$

Using the relationships between mass flow, engine pressure difference and altitude of Figure 2, and the Standard Atmosphere Model; the result was

$$C_{P23} \sim \sigma^a, \ a < 0 \qquad (6)$$

where σ is the Standard Atmosphere density ratio. However, Figure 23 implies

$$a > 0 \ ,$$

and therefore further analyses will await detailed mass flow measurements.

In Figure 24, the same installation parameters are presented for different level flight cruise power settings in terms of the resulting equivalent airspeeds. The indicated variation of pressure recovery and engine pressure difference with airspeed is believed,

at present, to be due to changes in the nacelle's external pressure distribution with angle-of-attack. As airspeed increases, angle-of-attack decreases and the flow static pressure on the lower surface of the nacelle will increase in the negative or "suction" direction.

It is evident from Figure 23 and 24, that, other than influencing engine pressure difference/mass flow characteristics, altitude exerts no significant effect on installation behavior. One thus can evaluate the aerodynamic characteristics of an installation configuration at any convenient altitude for flight test purposes.

The engine pressure difference data from Figure 24 were combined with engine cooling requirements and measured aircraft performance data to produce Figure 25. The altitude curves give the engine cooling requirements as a function of developed engine power for an ISA + 20°F day. The data were extropolated from cooling requirements for three different 540-series engines having different rated powers but identical mass flow/engine pressure difference characteristics. The data are for the same brake specific fuel consumption. The altitude curves were related to airspeed through power required data taken during the tests. Superimposed on the cooling requirements data are the engine pressure differnece results from Figure 24. Thus, Figure 25 presents a comparison of cooling requirements with the cooling effectiveness of different installation configurations (inlets), over the performance envelope of the aircraft. An important parameter which is missing from Figure 25 is the fuel-air mixture ratio which exerts a strong influence on cooling requirements. At present, however, sufficient cooling data is not available to incorporate this parameter into such a graphical presentation.

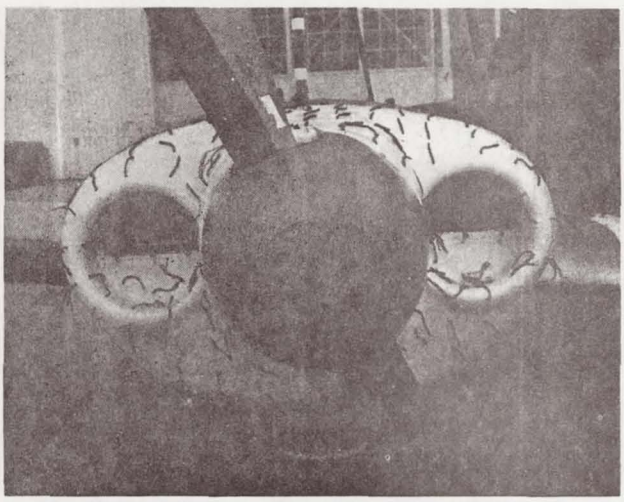

Fig. 20 - Post-flight view of the 0.3A inlet

Figure 25 offers an important conclusion regarding cooling which otherwise might be overlooked. Inadequate cooling can result from an aircraft not meeting design performance goals as well as poor installation design. The shift in the installation (inlets) cooling curves with configurations changes (0.3F, STD, 0.6F inlets) in Figure 25 is obvious. If the drag of the PA-41P were reduced, then these curves would shift vertically upward relative to the cooling requirement (altitude) curves to provide increased cooling effectiveness.

Figures 26 and 27 present direct comparisons of the four inlets tested. In Figure 26, the basis of comparison is the plenum pressure recovery. A boundary is defined below which pumping mechanisms, such as a cowl flap, would

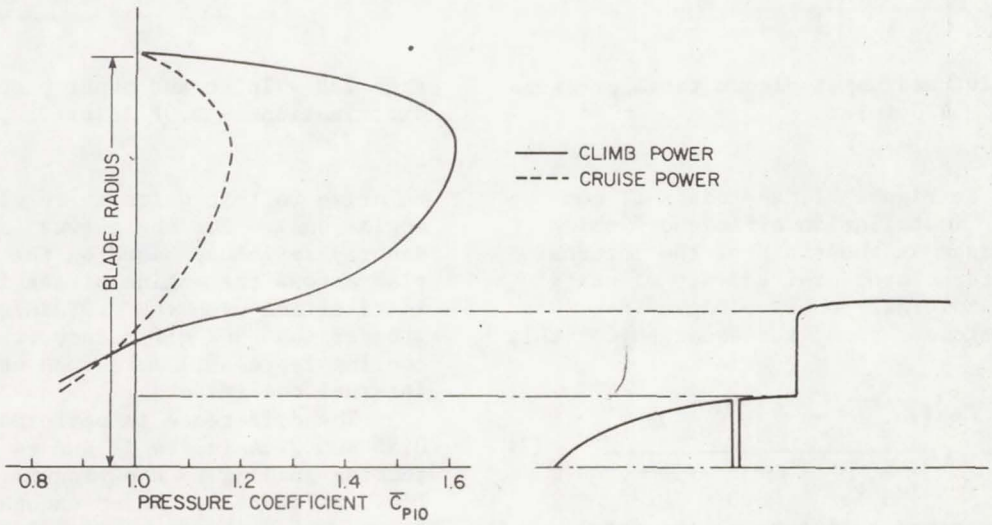

Fig. 21 - Propeller wake total pressure distributions

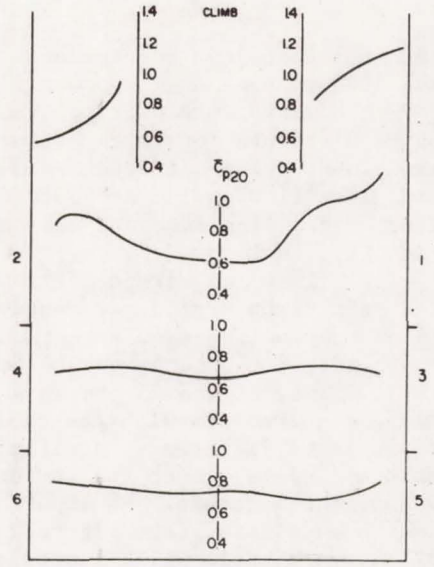

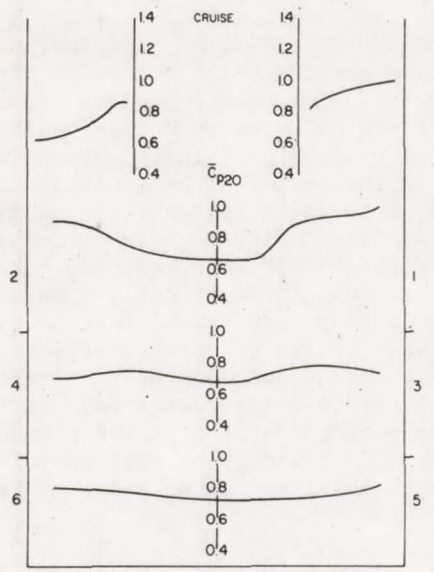

Fig. 22A - Inlet and upper plenum total pressure distributions - STD inlet

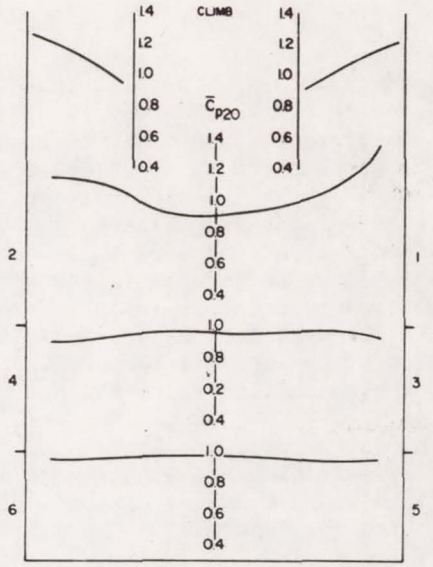

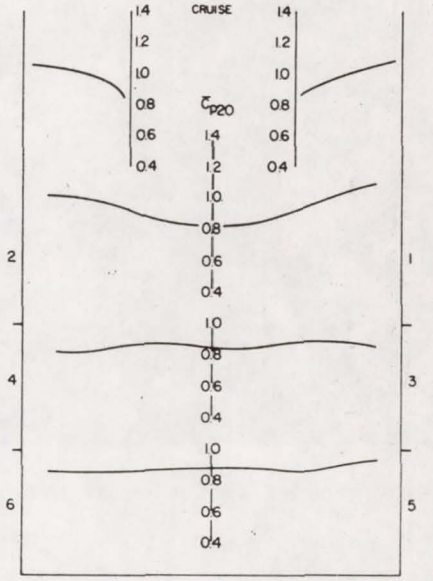

Fig. 22B - Inlet and upper plenum total pressure distributions - 0.3F inlet

be required. In Figure 27, the basis of comparison is an "installation efficiency" which is hereby defined as the ratio of the internal cooling drag for a pressure recovery of unity to the actual internal cooling drag. In pressure coefficient form, the equation for this efficiency is

$$\eta_{IP} = \frac{(\sqrt{\rho_3/\rho_o} - \sqrt{1 - C_{P23}})}{(\sqrt{\rho_3/\rho_o} - \sqrt{C_{P20} - C_{P23}})} \quad (7)$$

This parameter gives a measure of the total internal cooling drag of an installation relative to that which is required to cool the engine only. For the curves in Figure 27, the density ratio was based on the 130°F temperature rise across the engine at sea level. Only the installation with the 0.3F inlet achieves greater than 50% efficiency, that is, engine cooling represents more than one-half the total internal cooling drag.

The difference in performance between the 0.3F and 0.3A inlets is due to the internal ducting leading to the plenum. The 0.3F inlet, in Figure 8, is far enough forward that a reasonable duct can be fitted between the inlet throat and the plenum. The duct area

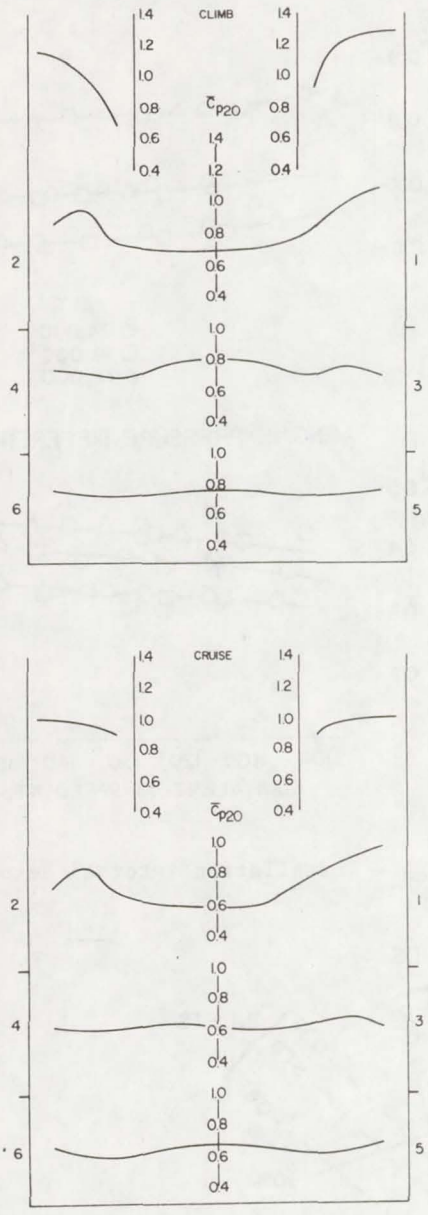

Fig. 22C - Inlet and upper plenum total pressure distributions - 0.3A inlet

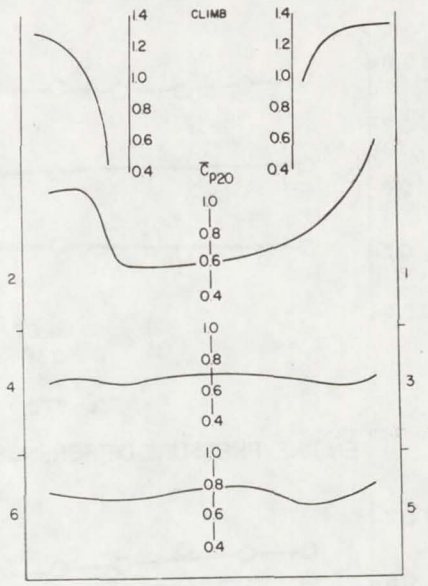

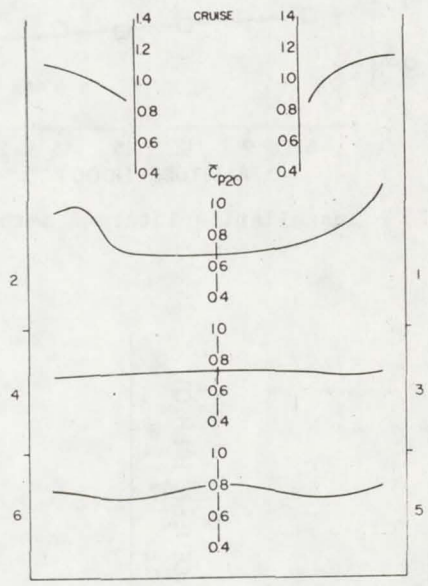

Fig. 22D - Inlet and upper plenum total pressure distributions - 0.6F inlet

increased rearward and some additional diffusion was accomplished here. In Figure 9, the 0.3A inlet leaves little room for a transition duct from throat to plenum. Although 0.3F and 0.3A are the same inlet shapes, the aft location forces the 0.3A inlet to function more like an orifice than a reasonable streamlined intake. Consequently, while both of these may be called inlets, only one functions efficiently as such; the other functions more like a "hole" with all aerodynamic connotations of such, applying.

The practical interpretations of these numbers are given in Figures 28 and 29. The velocity increments represent the cost of the internal cooling drag to aircraft performance. The data presented are for pressurized twins, and are based on published cruise performance values and respective engine cooling requirements. The velocity increments corresponding to pressure recovery and efficiency values of 1.0 represent the cost solely for cooling the engine. The additional costs for inlet and plenum losses follow from there.

CONTINUING PROGRAM

The results presented in this paper represent approximately 20% of the potential

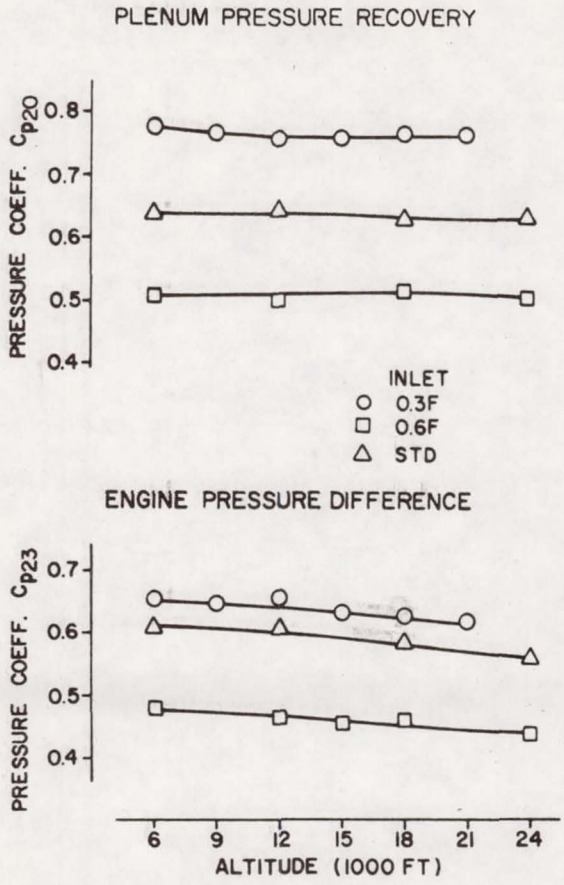

Fig. 23 - Installation internal aerodynamics - climb

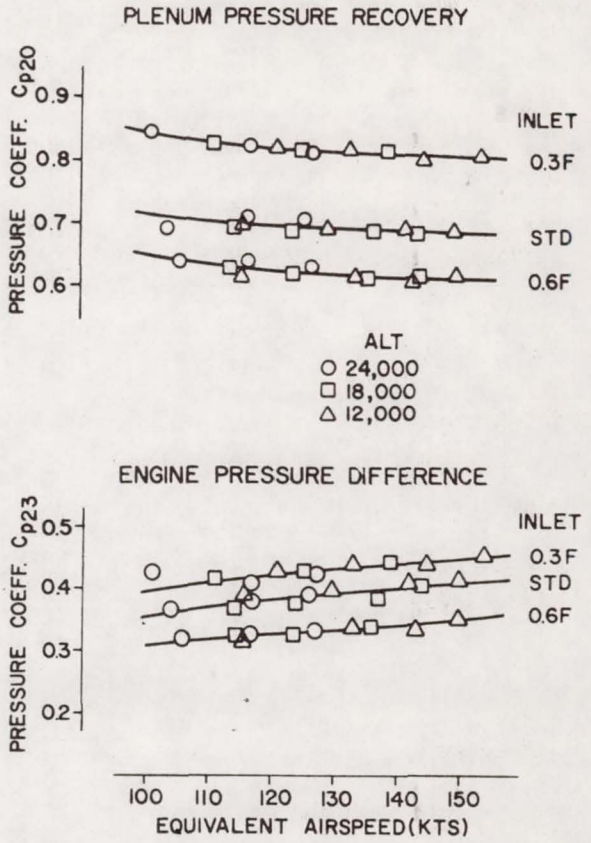

Fig. 24 - Installation internal aerodynamics - cruise

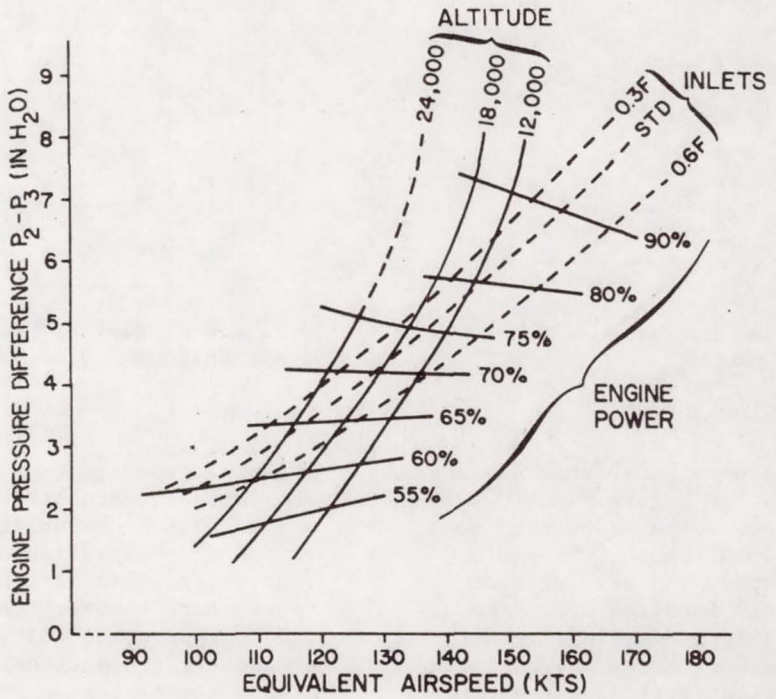

Fig. 25 - PA-41P engine cooling requirements, performance, and installation cooling effectiveness

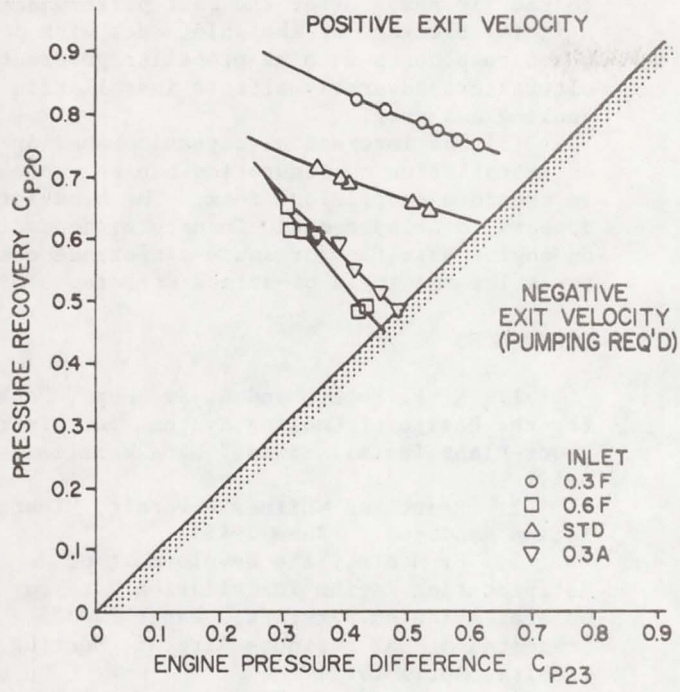

Fig. 26 - Inlet influence on plenum pressure recovery

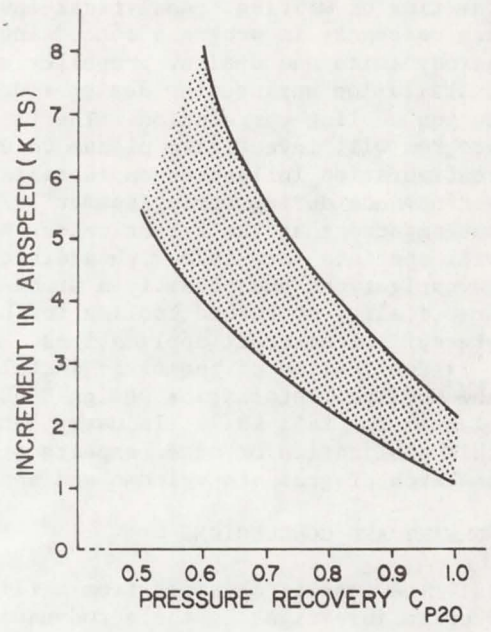

Fig. 28 - Plenum pressure recovery influence on aircraft performance for current pressurized twins

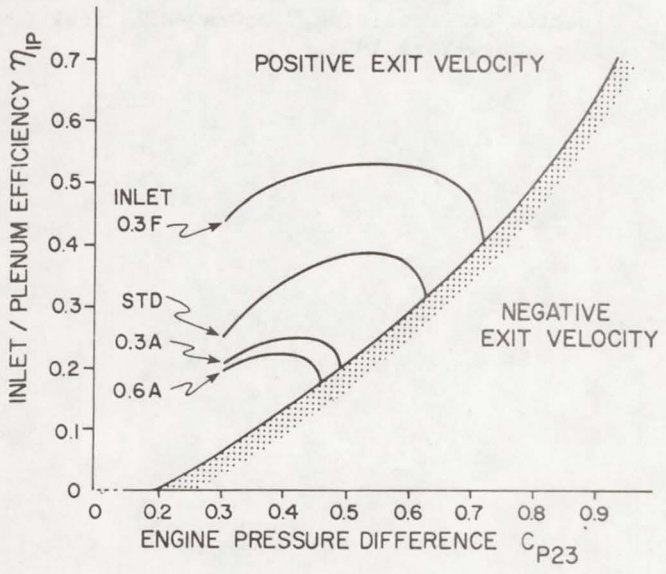

Fig. 27 - Inlet/plenum efficiency

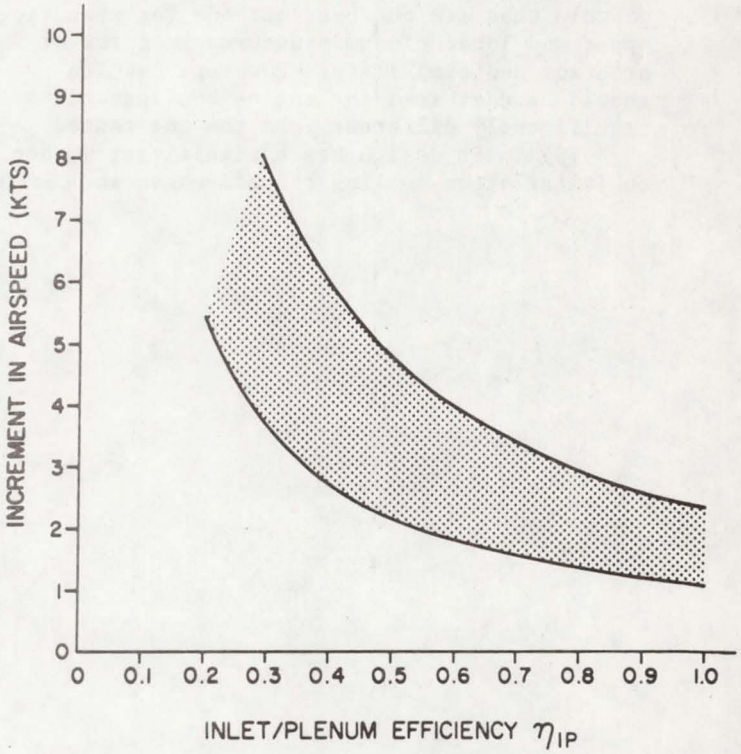

Fig. 29 - Inlet/plenum efficiency influence on aircraft performance for current pressurized twins

information contained in the data acquired at the time of writing. Analytical investigations are currently in progress concerning inlet aerodynamics and design, propeller effects, installation engineering design models, and engine cooling correlation. The flight research program will investigate plenum volume and exit configuration influences on installation performance during spring/summer 1977. It is anticipated that the flight research program will continue into 1978 with additional inlet investigations and possibly a study of the practicality of forced cooling for high altitude pressurized aircraft applications.

Publication of the first installments of the Cooling Installation Design Handbook are planned for fall 1977. Industry comments on this publication or other aspects of our research program are welcome and appreciated.

SUMMARY AND CONCLUSIONS

The results obtained from a flight research program investigating the aerodynamics of cooling installations which were presented in this paper support the following:

(1) Small plenum volumes associated with tightly cowled engines have flow velocities sufficiently high to affect engine face pressure measurement.

(2) The pressure belt, baffle button and piccolo tube are the best methods for measuring upper and lower plenum pressures in terms of accuracy and simplicity. However, caution should be exercised for engine configurations significantly different from the one tested.

(3) Inlet design has a significant impact on installation cooling effectiveness and cooling drag. Low velocity ratio inlets with attention to the lip shape offer the best performance.

(4) Blockage of the inlet duct with power-plant components such as propeller governors and alternators adversely affects installation cooling and drag.

(5) The internal aerodynamic behavior of an installation configuration can be represented in pressure coefficient form. The behavior appears to be systematic in nature; depending on engine mass flow/pressure difference characteristics and angle-of-attack effects.

REFERENCES

1. K. F. Rubert and G. S. Knopf, "A Method for the Design of Cooling Systems for Aircraft Power-Plant Installations," NACA Wartime Report L-491.

2. Pratt and Whitney Aircraft, "Installation Handbook." June 1945

3. F. Monts, "The Development of Reciprocating Engine Installation Data for General Aviation Aircraft," Paper 730325 presented at SAE Business Aircraft Meeting, Wichita, April 1973.

4. R. H. Lange, "A Summary of Drag Results from Recent Langley Full-Scale-Tunnel Tests of Army and Navy Airplanes," NACA Wartime Report L-108.

5. T. F. Hammen, Jr., and W. H. Rowley, "Factors Pertaining to Installation at Inverted, In-Line Aircooled Aircraft Engines," SAE Journal (Transactions), Vol. 54, No. 3, March 1946.

6. D. Kuchemann and J. Weber, "Aerodynamics of Propulsion," McGraw-Hill Book Co., Inc., New York 1953.

Society of Automotive Engineers, Inc.
400 COMMONWEALTH DRIVE, WARRENDALE, PA. 15096

24 page booklet. Printed in U.S.A.